Study on Crosstalk Between Space Transient Interference Microstrip Lines Using Finite Difference Time Domain Method

Y. X. Sun, Q. Li, W. H. Yu, Q. H. Jiang, and Q. K. Zhuo

College of Information and Communications Engineering
Harbin Engineering University, Harbin 150001, China
sunyaxiu@hrbeu.edu.cn, liqian_dianci@163.com, wenyu@2comu.com, clj1-1@163.com,
zhuoqingkun@hrbeu.eu.cn

Abstract ─ In the paper, a Carson reciprocity theorem-based numerical method is proposed to analyze the crosstalk of space transient interference microstrip lines. Firstly, the proposed method is realized via solving the coupling voltage between the space transient interference and the microstrip lines by the use of Carson reciprocity theorem. Then the crosstalk between the microstrip lines caused by the coupling voltage is studied based on the finite difference time domain (FDTD) method. Lastly, compared with the Baum-Liu-Tesche (BLT) equation method, the proposed method reduces the computational complexity without solving the complex scattering field. In this paper, coupling between a dipole and a microstrip line will be considered and its coupling model will be given. FDTD and the parasitic parameter model between the microstrip lines are used to get the crosstalk. In addition, the crosstalk between the microstrip lines caused by the space transient interference is analyzed in comparison with the impedance match and mismatch of the terminals. The simulated results show that the voltages of the reflection and crosstalk which are on the victim line with mismatched loads are larger than that with matched loads, and the fluctuate time of the signal on the victim line with mismatched loads is over two times than that with matched loads, which help to verify the effectiveness of the proposed method. Moreover, when we analyze the electromagnetic problems on the surface of the arbitrary shaped ideal conductor, the image method is unavailable because the surface of ideal conductor is not infinite, while the analytic method is unavailable either, on account of the boundary of the ideal conductor is irregular. So the conventional approach is difficult to solve the problems, but the proposed method can work well for the problems due to the fact that it has nothing to do with the boundary shape, and it is only connected with the source and its field. Therefore, the proposed method is suitable for a wide range.

Index Terms ─ Carson reciprocity theorem, crosstalk, FDTD, space transient interference.

I. INTRODUCTION

Printed circuit board has been widely applied to various kinds of electronic devices due to its small size and high integration. With the rapid development of integrated circuit technologies, the PCB has been developed to carry out the high density, high speed and multiple stratification, which may cause electromagnetic coupling in high frequency and signal integrity problems such as ringing, overshoot, and crosstalk and so forth, Among these signal integrity problems, crosstalk is one of the most serious issues, which has been widely studied.

Crosstalk has been extensively researched and reported [1-8]. Shahid studied on the model structures inside the coupled microstrip lines and their correlation with crosstalk between the microstrip lines by using FDTD and singular value decomposition methods [4]. Lee and Jung investigated the crosstalk in parallel high speed interfaces [5].

However, the space electromagnetic interference is ignored in these reported results. The coupling between the space electromagnetic interference and transmission lines has been discussed [9-13]. A coupling analysis method is proposed based on the BLT equation to study the coupling terminal response between electromagnetic wave and microstrip line [9]. The time-domain variant of generalized telegrapher equations for transient electromagnetic coupling is proposed to analyze a finite-length wire above a lossy half-space [10]. Transmission line (TL) applied in lightning electromagnetic field coupling has been reported [13]. However, these proposed methods have a high computational complexity. And then the researchers carried on the further research about this problem [14-19]. Pual proposed a SPICE model that is used to predict the voltage and currents of the multiconductor transmission line (MTL) excited by an electromagnetic field [14]. Gad proposed a new algorithm to analyze the electromagnetic (EM) coupling for non-uniform multiconductor

Submitted On: January 5, 2015
Accepted On: June 4, 2015

transmission lines based on Maxwell equations [15]. Canavero gave an efficient iterative solution in the frequency domain for electromagnetic pulse (EMP) coupling to multiconductor transmission line (MTL) based on distributed analytic representation [16]. However, the crosstalk between microstrip lines caused by the coupling voltage has not been discussed in these researches.

For these reasons, a new method is proposed to calculate the crosstalk caused by the coupling voltage between space transient interference and transmission lines on the basis of the Carson reciprocity theorem. The proposed method avoids calculating the complex scattering field, which reduces the computational complexity. Moreover, the proposed method is effective to deal with the complex boundary. We get the crosstalk voltage between the microstrip lines by the use of FDTD and the parasitic parameter mode. In addition, the space transient interference of the microstrip lines is discussed in comparison with the impedance match and mismatch of the terminals. The simulated results show that the voltage of the reflection and crosstalk on the victim line with mismatched loads are larger than that with matched loads, and the fluctuate time of the signal on the victim line with mismatched loads is over two times than it with matched loads, which help to verify the accuracy of the proposed method.

II. SPACE TRANSIENT INTERFERENCE AND MICROSTRIP LINES COUPLING ANALYSIS BASED ON CARSON RECIPROCITY THEOREM

Carson reciprocity theorem has been used to describe the relationship between the two different fields, which are given by two different field sources. A typical example shown in Fig. 1 is considered to discuss the Carson reciprocity theorem. Here, we consider a volume Ω, which is filled with linear dielectric. Additionally, two current source $\vec{J}_a$ and $\vec{J}_b$ are distributed in the sub-volumes Ω_2 and Ω_1. The electric field and magnetic field are $\vec{E}_a$, $\vec{H}_a$ and $\vec{E}_b$, $\vec{H}_b$ respectively.

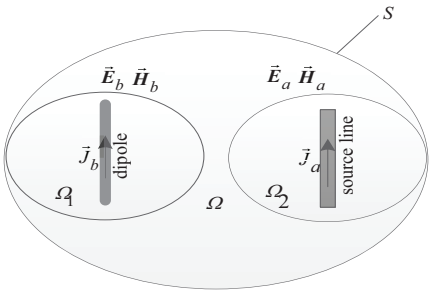

Fig. 1. Description of Carson reciprocity theorem.

According to the vector equation:

$$\nabla\cdot(\vec{A}\times\vec{B})=\vec{B}\cdot(\nabla\times\vec{A})-\vec{A}\cdot(\nabla\times\vec{B}), \tag{1}$$

where $\vec{A}$ and $\vec{B}$ are the arbitrary vectors. Combining Fig. 1 with formula (1), we can get the following equations in Ω:

$$\nabla\cdot(\vec{E}_a\times\vec{H}_b)=\vec{H}_b\cdot(\nabla\times\vec{E}_a)-\vec{E}_a\cdot(\nabla\times\vec{H}_b), \tag{2}$$

$$\nabla\cdot(\vec{E}_b\times\vec{H}_a)=\vec{H}_a\cdot(\nabla\times\vec{E}_b)-\vec{E}_b\cdot(\nabla\times\vec{H}_a). \tag{3}$$

According to the Maxwell equations in frequency domain, we can obtain:

$$\begin{cases}\nabla\times\vec{E}=-\mathrm{j}w\mu\vec{H}\\ \nabla\times\vec{H}=\vec{J}+\mathrm{j}w\varepsilon\vec{E}\end{cases}. \tag{4}$$

On the basis of the Maxwell equation and the formula (2), (3), we get:

$$\nabla\cdot[(\vec{E}_a\times\vec{H}_b)-(\vec{E}_b\times\vec{H}_a)]=\vec{E}_b\cdot\vec{J}_a-\vec{E}_a\cdot\vec{J}_b, \tag{5}$$

where $\vec{J}_a$ is the current source of source line, and $\vec{J}_b$ is the current source of the dipole. Considering formula (5) and Gaussian theorem, we get:

$$\oint_S[(\vec{E}_a\times\vec{H}_b)-(\vec{E}_b\times\vec{H}_a)]\cdot dS=\int_\Omega(\vec{E}_b\cdot\vec{J}_a-\vec{E}_a\cdot\vec{J}_b)\,d\Omega. \tag{6}$$

In formula (6), S is the boundary of Ω. When Ω is an infinite space, S can be regarded as an infinite surface of a sphere. Thus, the electromagnetic wave on S is TEM wave, which satisfies $\vec{E}=Z\vec{H}\times\vec{e}_r$, where Z is wave impedance and $\vec{e}_r$ is unit vector. Then, the integration of left hand of formula (6) is zero. Thus, the right hand of formula (6) can be written as:

$$\int_\Omega\vec{E}_b\cdot\vec{J}_a d\Omega=\int_\Omega\vec{E}_a\cdot\vec{J}_b d\Omega, \tag{7}$$

which is the so called Carson reciprocity theorem equation. In order to better understand the coupling between microstrip lines and space transient interference, a model of microstrip line marked as source line and interference source dipole is built as shown in Fig. 2.

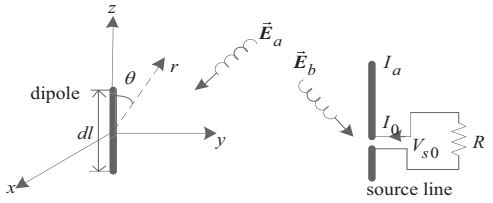

Fig. 2. Coupling model between the dipole and the source line.

The far field of the dipole is expressed as:

$$\vec{E}_b=\frac{j\omega\mu}{4\pi r}(I_b d\vec{l})e^{-jkr}\sin\theta. \tag{8}$$

Then, according to the Fig. 2, the coupling voltage on the source line caused by the dipole is below:

$$V_{s0} = \frac{1}{I_0}\int_l \vec{\boldsymbol{E}}_b \cdot I_a d\vec{l}, \tag{9}$$

where I_0 is the inspiriting current, when the source line acts as the emission antenna, I_a is the current distribution in the emission antenna. After that, we have:

$$V_{s0} = \frac{1}{I_0}\int_\Omega \vec{\boldsymbol{E}}_b \cdot \vec{\boldsymbol{J}}_a d\Omega, \tag{10}$$

where $I_b d\vec{l} = \vec{\boldsymbol{J}}_b d\Omega$ is used in (10). Considering Carson reciprocity theorem, we have:

$$V_{s0} = \frac{1}{I_0}\int_\Omega \vec{\boldsymbol{E}}_a \cdot \vec{\boldsymbol{J}}_b d\Omega, \tag{11}$$

and

$$\vec{\boldsymbol{J}}_b = \vec{\boldsymbol{E}}_b \frac{4\pi r}{j\omega\mu} e^{jkr} \frac{1}{d\Omega} \sin^{-1}\theta. \tag{12}$$

Based on (11) and (12), we have:

$$V_{s0} = \frac{1}{I_0}\vec{\boldsymbol{E}}_a \cdot \vec{\boldsymbol{E}}_b \frac{4\pi r}{j\omega\mu} e^{jkr} \sin^{-1}\theta. \tag{13}$$

By using (13), the coupling voltage V_{s0} between the source line and the dipole can be obtained.

III. CROSSTALK ANALYSIS ON MICROSTRIP LINES USING FDTD

In this section, V_{s0} is added to a homogeneous and loss-less microstrip line, as shown in Fig. 3. Here, the port 1 is excited by V_{s0}, while other ports are terminated with the linear loads. Port2, port3 and port4 are terminated with R_{L0}, R_1 and R_2 respectively. The voltage and current of the homogeneous and loss-less parallel microsrip lines meet the following telegraph equations:

$$\frac{\partial \boldsymbol{V}(z,t)}{\partial z} = -\boldsymbol{L}(z)\frac{\partial \boldsymbol{I}(z,t)}{\partial t}, \tag{14}$$

$$\frac{\partial \boldsymbol{I}(z,t)}{\partial z} = -\boldsymbol{C}(z)\frac{\partial \boldsymbol{V}(z,t)}{\partial t}. \tag{15}$$

Then combine the boundary equations of the parallel microstrip lines with the telegraph equations we can obtain the crosstalk voltage.

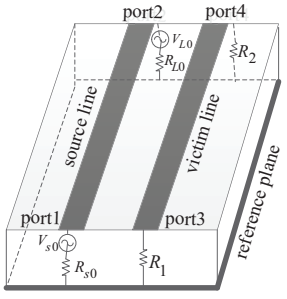

Fig. 3. Model of microstrip lines with coupling voltage V_{s0}.

Taking the FDTD into consideration, the discrete model of the microstrip lines is shown in Fig. 4, where:

$$\boldsymbol{V}_s = \begin{bmatrix} V_{s0} \\ 0 \end{bmatrix}, \quad \boldsymbol{R}_s = \begin{bmatrix} R_{s0} & 0 \\ 0 & R_1 \end{bmatrix},$$

$$\boldsymbol{V}_L = \begin{bmatrix} V_{L0} \\ 0 \end{bmatrix}, \quad \boldsymbol{R}_L = \begin{bmatrix} R_{L0} & 0 \\ 0 & R_2 \end{bmatrix}.$$

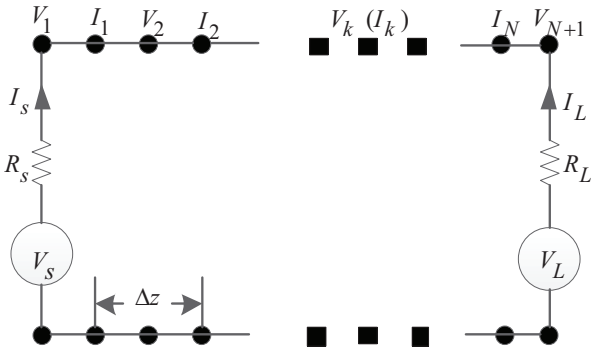

Fig. 4. Discrete model of the microstrip lines based on FDTD method.

Then, combine the Fig. 4 with the formula (15) we get the difference equations at the source end and load end as shown in formula (16), (17) respectively:

$$\frac{1}{\Delta z}(\boldsymbol{I}_1^{n+\frac{1}{2}} - \boldsymbol{I}_0^{n+\frac{1}{2}}) + \frac{1}{\Delta t}\boldsymbol{C}(\boldsymbol{V}_1^{n+1} - \boldsymbol{V}_1^{n}) = 0, \tag{16}$$

$$\frac{1}{\Delta z}(\boldsymbol{I}_{N+1}^{n+\frac{1}{2}} - \boldsymbol{I}_N^{n+\frac{1}{2}}) + \frac{1}{\Delta t}\boldsymbol{C}(\boldsymbol{V}_{N+1}^{n+1} - \boldsymbol{V}_{N+1}^{n+1}) = 0. \tag{17}$$

By considering the average $\boldsymbol{I}_0$ and $\boldsymbol{I}_{N+1}$, we have:

$$\frac{1}{\Delta z}(\boldsymbol{I}_1^{n+\frac{1}{2}} - \frac{\boldsymbol{I}_s^{n+1} + \boldsymbol{I}_s^{n}}{2}) + \frac{1}{\Delta t}\boldsymbol{C}(\boldsymbol{V}_1^{n+1} - \boldsymbol{V}_1^{n}) = 0, \tag{18}$$

$$\frac{1}{\Delta z}(\frac{\boldsymbol{I}_L^{n+1} + \boldsymbol{I}_L^{n}}{2} - \boldsymbol{I}_N^{n+\frac{3}{2}}) + \frac{1}{\Delta t}\boldsymbol{C}(\boldsymbol{V}_{N+1}^{n+1} - \boldsymbol{V}_{N+1}^{n}) = 0. \tag{19}$$

From the discussions above, the boundary equations at source end and load end as shown in formula (20), (21) respectively:

$$\boldsymbol{V}_1^{n+\frac{1}{2}}(t) = \boldsymbol{V}_s^{n+\frac{1}{2}}(t) - \boldsymbol{R}_s\boldsymbol{I}_s^{n+\frac{1}{2}}(t), \tag{20}$$

$$\boldsymbol{V}_{N+1}^{n+\frac{1}{2}}(t) = \boldsymbol{V}_L^{n+\frac{1}{2}}(t) - \boldsymbol{R}_L\boldsymbol{I}_L^{n+\frac{1}{2}}(t). \tag{21}$$

Then we have:

$$\frac{\boldsymbol{V}_1^{n+1} + \boldsymbol{V}_1^{n}}{2} = \frac{\boldsymbol{V}_s^{n+1} + \boldsymbol{V}_s^{n}}{2} - \boldsymbol{R}_s\frac{\boldsymbol{I}_s^{n+1} + \boldsymbol{I}_s^{n}}{2}, \tag{22}$$

$$\frac{\boldsymbol{V}_{N+1}^{n+1} + \boldsymbol{V}_{N+1}^{n}}{2} = \frac{\boldsymbol{V}_L^{n+1} + \boldsymbol{V}_L^{n}}{2} - \boldsymbol{R}_L\frac{\boldsymbol{I}_L^{n+1} + \boldsymbol{I}_L^{n}}{2}. \tag{23}$$

From the equations (18), (22) and (19), (23), we can obtain the following iterative equations of $\boldsymbol{V}_1$ and $\boldsymbol{V}_{N+1}$:

$$\begin{aligned}\boldsymbol{V}_1^{n+1} = {} & (\frac{\Delta z}{\Delta t}\boldsymbol{R}_s\boldsymbol{C} + \boldsymbol{E})^{-1}[(\frac{\Delta z}{\Delta t}\boldsymbol{R}_s\boldsymbol{C} - \boldsymbol{E})\boldsymbol{V}_1^{n} - \\ & 2\boldsymbol{R}_s\boldsymbol{I}_1^{n+\frac{1}{2}} + (\boldsymbol{V}_s^{n+1} + \boldsymbol{V}_s^{n})],\end{aligned} \tag{24}$$

$$\boldsymbol{V}_{N+1}^{\,n+1}=(\frac{\Delta z}{\Delta t}\boldsymbol{R}_L\boldsymbol{C}+\boldsymbol{E})^{-1}[(\frac{\Delta z}{\Delta t}\boldsymbol{R}_L\boldsymbol{C}-\boldsymbol{E})\boldsymbol{V}_{N+1}^{\,n}+ 2\boldsymbol{R}_L\boldsymbol{I}_N^{\,n+\frac{1}{2}}+(\boldsymbol{V}_L^{\,n+1}+\boldsymbol{V}_L^{\,n})], \quad (25)$$

where $\boldsymbol{C}$ and $\boldsymbol{L}$ are the distributed parameter matrices and $\boldsymbol{E}$ is identity matrix. From (14) and (15), the iterative equations of voltage and current at k segment are:

$$\boldsymbol{V}_k^{\,n+1}=\boldsymbol{V}_k^{\,n}-\frac{\Delta t}{\Delta z}\boldsymbol{C}^{-1}(\boldsymbol{I}_k^{\,n+\frac{1}{2}}-\boldsymbol{I}_{k-1}^{\,n+\frac{1}{2}}) \quad k=2,3,.....N, \quad (26)$$

$$\boldsymbol{I}_k^{\,n+\frac{3}{2}}=\boldsymbol{I}_k^{\,n+\frac{1}{2}}-\frac{\Delta t}{\Delta z}\boldsymbol{L}^{-1}(\boldsymbol{V}_{k+1}^{\,n+1}-\boldsymbol{V}_k^{\,n+1}) \quad k=1,....N, \quad (27)$$

where Δt is the temporal offset and Δz is the spatial offset, which should satisfy $\Delta t \le \frac{\Delta z}{c}$ and c is the speed of light.

IV. NUMERICAL RESULTS

In this section, the performance of the proposed method is verified in comparison with Carson reciprocity theorem and BLT. To show the performance of the Carson reciprocity theorem, coupling voltage in the time domain is studied and compared with BLT. We get the BLT equations of the load voltage:

$$\begin{bmatrix}V_{s0}\\V_{L0}\end{bmatrix}=\begin{bmatrix}1+\rho_1 & 0\\0 & 1+\rho_2\end{bmatrix}\begin{bmatrix}-\rho_1 & e^{\gamma l}\\e^{\gamma l} & -\rho_2\end{bmatrix}^{-1}\begin{bmatrix}S_1\\S_2\end{bmatrix}. \quad (28)$$

In the equation, Z_0 is the characteristic impedance and γ is the propagation constant of the microstip line, $\rho_1=\frac{R_{s0}-Z_0}{R_{s0}+Z_0}$, $\rho_2=\frac{R_{L0}-Z_0}{R_{L0}+Z_0}$. In this paper, we consider the ρ_1 and ρ_2 are zero, then we can get the $V_{s0}=\frac{S_2}{e^{\gamma l}}$. While according to the Agrawal model, we can solve:

$$S_2=-\frac{1}{2}\int_0^l e^{\gamma(l-x)}[V_s^{'}(\mathrm{x})-Z_0 I_s^{'}(\mathrm{x})]dx = e^{\gamma l}\frac{[e^{-(\gamma+jk)l}-1](Z_0+\frac{j\omega\mu}{120\pi})\vec{E}_b d}{2(\gamma+jk)}, \quad (29)$$

where

$$V_s^{'}=\vec{E}_x^{inc}(x,d)-\vec{E}_x^{inc}(x,0), \quad (30)$$

and

$$I_s^{'}=-j\omega c\int_0^l \vec{E}_z^{inc}(x,z)dz. \quad (31)$$

Here, $\vec{E}_x^{inc}$ and $\vec{E}_z^{inc}$ are the components of $\vec{E}_b$ in the x direction and z direction. l is the length of the microstrip line, d is the distance from the microstrip line to the reference plane, $k=\omega/\mathrm{c}$. Then,

$$V_{s0}=\frac{[e^{-(\gamma+jk)l}-1](Z_0+\frac{j\omega\mu}{120\pi})\vec{E}_b d}{2(\gamma+jk)}. \quad (32)$$

We make Fourier inversion for equations (13) and (32), and then we can get the waveform figure in time domain as shown in Fig. 5.

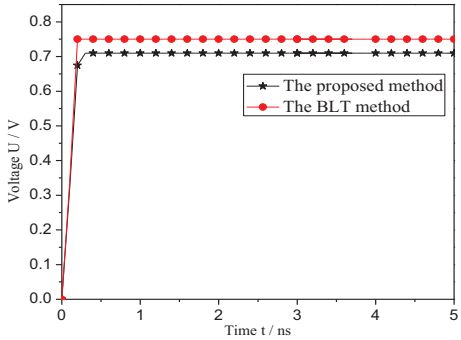

Fig. 5. Coupling voltage characteristics.

It is found from Fig. 5 that, the trend of the voltages between Carson reciprocity theorem and the BLT methods are coincident, but there is a little bit difference in the value of the voltage between the proposed method and the BLT method. As shown in formula (32), when we solve the coupling voltage V_{s0} with the BLT method, it is only considering the coupling from the field $\vec{E}_b$ to the microstrip line without considering the radiation field $\vec{E}_a$ caused by the current on the microstrip line. While the proposed method considered it. So the Carson reciprocity theorem method is more accurate to solve the coupling between space transient interference and microstrip lines. Moreover, we can see the BLT method has a complex calculation from formula (29) and (32). Since the radiation of dipole is spherical wave, the current distribution on the microstrip lines caused by the dipole is shown in Fig. 6. The line on the left side is the source line, and the right one is the victim line. It is observed that the crosstalk exists on the microstrip lines.

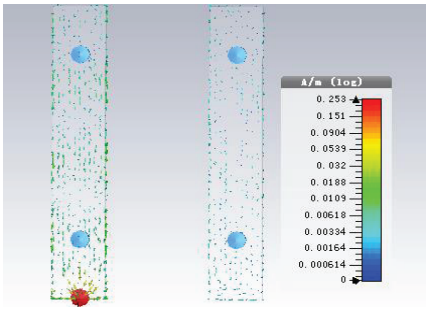

Fig. 6. Surface current distribution on the microstrip lines excited by dipole.

In the simulation, the substrate was FR4 with a relative permittivity of 4.7, loss tangent of 0.002, and substrate thickness of 1.5 mm. We set $\Delta t = 10^{-11}$s and $\Delta z = 3*10^{-3}$ m. The maximum time step was $t_{max} = 500$ in the FDTD simulation. The length of the parallel microstrip lines is set as 6 cm and the width of the microstrip lines is set as 1 mm. The distance between the two microstrip lines is 2 mm and the thickness of the microstrip lines is set as 1.4 mm. The distributed parameter matrices are:

$$\boldsymbol{L} = \begin{bmatrix} 309 & 21.7 \\ 21.7 & 309 \end{bmatrix} nH/m, \tag{33}$$

and

$$\boldsymbol{C} = \begin{bmatrix} 144 & -6.4 \\ -6.4 & 144 \end{bmatrix} pF/m. \tag{34}$$

Example 1: *All the ports with matched loads*

To solve the near-end crosstalk (NEXT) and the far-end crosstalk (FEXT) between the source line and victim lines, all the ports were matched with 50 Ω linear loads in this example. The simulated voltage of the source line was shown in Fig. 7. It can be seen that the signal transmission period on the source line without distortion is $\frac{6\times10^{-2}m}{1.524\times10^{8}m/s} = 3.9\times10^{-10}s = 0.39ns.$

Then according to the voltage of the source line, we get the voltage distribution of the victim line at near-end and far-end with HyperLynx software and Carson reciprocity theorem method as shown in Fig. 8 and Fig. 9, respectively. We can see the trend of the voltages distribution is accordant between the Carson reciprocity theorem and the HyperLynx software. This indicates that the proposed method is effective to analyze the crosstalk between the microstrip lines. But we can see the voltage appearing with fluctuation at the near-end and far-end with the Carson reciprocity theorem method, which is the meshing sparseness when we solve the voltage with the proposed method. It can be improved by increasing the grid. Then we analyzed the crosstalk of all ports with mismatched loads based on the proposed method as shown in Example 2.

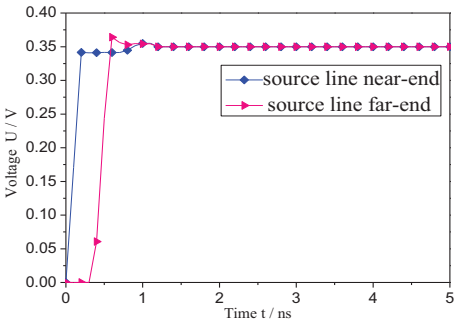

Fig. 7. Voltage distribution of source line.

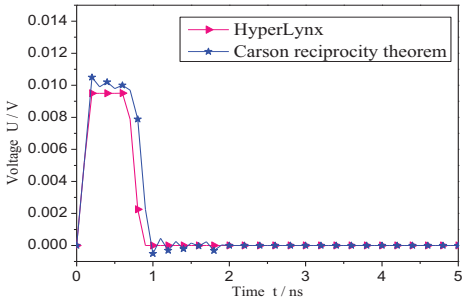

Fig. 8. Voltage distribution of victim line at near-end.

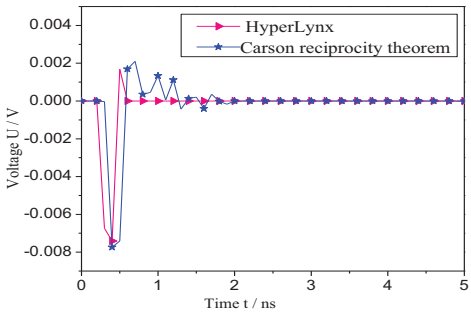

Fig. 9. Voltage distribution of victim line at far-end.

Example 2: *All ports with mismatched loads*

In this experiment, the port1 was 100 Ω, the port2 was 150 Ω, the port3 was 120 Ω and port4 was 300 Ω. The voltage of the source line and victim line were described in Fig. 10 and Fig. 11. We can see that the signal appears with serious reflection on source line in Fig. 10. In Fig. 11, the signal on victim line appeared seriously fluctuate, which is not only caused by the mismatched loads, but also caused by the crosstalk voltage from the source line. The waveform in Fig. 11 is formed by the overlap of the reflection and the crosstalk, which tends to be stable after 4 ns. It is two times longer than that in Fig. 8 and Fig. 9. Thus, we can see that the loads play a great role in the reflection and crosstalk. Additionally, if we cannot make all the ports with matched load, it can effectively reduce the reflection and crosstalk by making the source end with matched load, in the design of system.

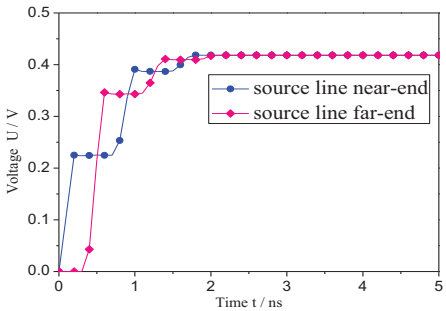

Fig. 10. Voltage distribution of source line.

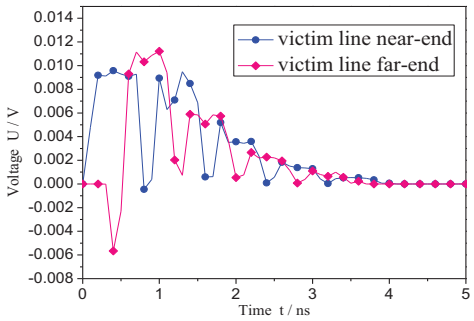

Fig. 11. Voltage distribution of victim line.

V. CONCLUSION

A new method has been proposed and investigated by using the Carson reciprocity theorem to calculate the coupling between the space transient interference and microstrip lines. We get the coincident trend in comparison with the proposed method and BLT. However, the proposed method avoids analyzing the complex scattered field, which reduces the computational complexity. Combining Carson reciprocity theorem and FDTD, we have discussed the crosstalk performance caused by the coupling voltages on the source line. Simulation results demonstrated that the voltages of the reflection and crosstalk which are on the victim line with mismatched loads are larger than that with matched loads, and the fluctuate time of the signal on the victim line with mismatched loads is over two times than it with matched loads. So the space transient interference can cause serious reflection and crosstalk. The simulation results are significant in devising systems to reduce crosstalk, reflection and enhance signal integrity.

ACKNOWLEDGMENTS

This work was supported by the National Nature Science Foundation of China under Grant 51209055, the Fundamental Research Funds for the Central Universities of China (HEUCF150818), the China Postdoctoral Science Foundation Funded Project (3236310246) and the Heilongjiang Science Funded (F2015028).

REFERENCES

[1] T. B. Jan, "Wavelet-based approach to evaluation of signal integrity," *IEEE Transaction on Industrial Electronics*, vol. 60, pp. 4590-4598, 2013.

[2] J. K. Du, "Analysis of coupling effects to PCB inside wave guide using the modified BLT equation and full-wave analysis," *IEEE Transaction on Microwave Theory and Techniques*, vol. 61, pp. 3514-3523, 2013.

[3] E. Song, "Modeling and design optimization of a wide-band passive equalizer on PCB based on near-end crosstalk and reflections for high-speed serial data transmission," *IEEE Transaction on Electromagnetic Compatibility*, vol. 52, pp. 410-420, 2010.

[4] A. Shahid, "Finite-difference time-domain analysis of electromagnetic modes inside printed coupled lines and quantification of crosstalk," *IEEE Transaction on Electromagnetic Compatibility*, vol. 51, pp. 1026-1033, 2009.

[5] K. Lee and H. K. Jung, "Serpentine microstrip lines with zero far-end crosstalk for parallel high-speed DRAM interfaces," *IEEE Transaction on Advanced Packaging*, vol. 33, pp. 552-558, 2010.

[6] M. Shin, "A wide-band passive equalizer design on PCB based on near-end crosstalk and reflections for 12.5 Gbps serial data transmission," *IEEE Microwave and Wireless Components Letters*, vol. 18, pp. 794-796, 2008.

[7] F. Buesink, "Overview of signal integrity and EMC design technologies on PCB: fundamentals and latest progress," *IEEE Transaction on Electromagnetic Compatibility*, vol. 55, pp. 624-638, 2013.

[8] Y. Peerawut, "Lightning-induced voltage over lossy ground by a hybrid electromagnetic circuit model method with cooray–rubinstein formula," *IEEE Transaction on Electromagnetic Compatibility*, vol. 51, pp. 975-985, 2009.

[9] Q. Peng, "Electromagnetic coupling terminal response for microstrip line based on BLT equation," *High Power Laser and Particle Beams*, vol. 25, pp. 1241-1246, 2013.

[10] D. Poljak, "Time-domain generalized telegrapher's equations for the electromagnetic field coupling to finite length wires above a lossy ground," *IEEE Transaction on Electromagnetic Compatibility*, vol. 54, pp. 218-223, 2012.

[11] F. Rachidi, "A review of field-to-transmission line coupling models with special emphasis to lightning-induced voltages on overhead lines," *IEEE Transaction on Electromagnetic Compatibility*, vol. 54, pp. 898-911, 2012.

[12] M. Brignone, "An effective approach for high-frequency electromagnetic field-to-line coupling analysis based on regularization techniques," *IEEE Transaction on Electromagnetic Compatibility*, vol. 54, pp. 1289-1297, 2012.

[13] M. Paolone, "Lightning electromagnetic field coupling to overhead lines: theory numerical simulations and experimental validation," *IEEE Transaction on Electromagnetic Compatibility*, vol. 51, pp. 532-547, 2009.

[14] C. R Pual, "A SPICE medal for multiconductor transmission lines excited by an incident electromagnetic field," *IEEE Transaction on Electromagnetic Compatibility*, vol. 32, pp. 342-

354, 1994.

[15] E. Gad, "Circuit-based analysis of electromagnetic field coupling with no uniform transmission lines," *IEEE Transaction on Electromagnetic Compatibility*, vol. 50, pp. 149-165, 2008.

[16] F. G. Canavero, "Analytic iterative solution of electromagnetic pulse coupling to multiconductor transmission lines," *IEEE Transaction on Electromagnetic Compatibility*, vol. 55, pp. 451-466, 2013.

[17] S. A. Pignari, "Plane-wave coupling to a twisted-wire pair above ground," *IEEE Transaction on Electromagnetic Compatibility*, vol. 53, pp. 508-523, 2011.

[18] A. Amedeo, "Electromagnetic coupling of lightning to power lines: transmission-line approximation versus full-wave solution," *IEEE Transaction on Electromagnetic Compatibility*, vol. 53, pp. 421-428, 2011.

[19] L. Qi, "Calculation of interference voltage on the nearby underground metal pipeline due to the grounding fault on overhead transmission lines," *IEEE Transaction on Electromagnetic Compatibility*, vol. 55, pp. 965-975, 2013.